

Long-span hybrid precast concrete bridge girder using ultra-high-performance concrete and normalweight concrete

Vidya Sagar Ronanki, Sriram Aaleti, and J. P. Binard

- Longer spans for prestressed concrete bridge girders demand larger prestressing forces, which can lead to reinforcement congestion at the ends of the girders and increased cracking.
- This paper proposes a hybrid girder concept using ultra-high-performance concrete (UHPC) in the end zones of traditional girder shapes with normalweight concrete (NWC) to solve the problems associated with larger prestressing forces.
- Experimental studies were conducted to investigate the shear and flexural behavior of the UHPC-to-NWC interface, and the results were used to calibrate a finite element analysis model of a full-scale long-span hybrid girder.
- The results showed that the hybrid girder reduced the amount of shear and end zone reinforcement required and improved end zone cracking performance.

Nearly 39% of bridges in the United States are 50 years old or older, with more than 10.4% of bridges listed as structurally deficient and more than 13% rated functionally obsolete.¹ The condition of the aging infrastructure, along with the continuous increase in traffic volume on roadways and waterways, creates a demand for highly durable bridge replacement solutions. These solutions need to be economical and must be implemented using rapid or accelerated construction methods. For more than 60 years, prestressed concrete girders have been used effectively across the United States because of their durability, low life-cycle cost, and modularity, among other advantages. Prestressed concrete girders are most commonly used for full-length, simply supported bridges. The standard I-shaped and bulb-tee precast concrete girder sections designed and fabricated in lengths up to 160 ft (49 m) constitute approximately one-third of the bridges built in the United States.² Long-span prestressed concrete bridge girders can be an effective bridge replacement solution. These girders can meet the economic, aesthetic, and environmental considerations of a project by reducing the number of girder lines and substructure units in bridge systems.

To increase the prestressed concrete girder span lengths and girder spacing, many state departments of transportation (DOTs) have used different methods, such as developing new shapes or modifying girder cross sections to accommodate more prestressing strands or facilitate splicing technology and segmental construction. Splicing technology is not widely used by state DOTs because of a lack of experienced

PCI Journal (ISSN 0887-9672) V. 64, No. 6, November–December 2019.

PCI Journal is published bimonthly by the Precast/Prestressed Concrete Institute, 200 W. Adams St., Suite 2100, Chicago, IL 60606.

Copyright © 2019, Precast/Prestressed Concrete Institute. The Precast/Prestressed Concrete Institute is not responsible for statements made by authors of papers in *PCI Journal*. Original manuscripts and discussion on published papers are accepted on review in accordance with the Precast/Prestressed Concrete Institute's peer-review process. No payment is offered.

local contractors and the need for more rigorous analysis during the design phase compared with traditional construction. Incorporating high-strength concrete and larger-diameter strands (such as 0.6 and 0.7 in. [15.2 and 17.8 mm] diameter strands) is another method owners use to increase efficiency. For example, state DOTs, such as those in Nebraska (NU girder), Florida (Florida I-beam [FIB]), Virginia (precast concrete economical fabrication [PCEF] girder), and Washington (WF100G girder), have developed new or modified I-shaped girders for spans ranging from 170 to 200 ft (52 to 61 m) with 6 to 8 ft (1.8 to 2.4 m) girder spacing. These new girders can be as deep as 100 in. (2.54 m) (in the case of WF100G) and accommodate more than ninety 0.6 in. diameter strands. Field observations indicate that the increased prestressing forces required for longer spans or larger girder spacing can lead to problems, especially related to end zone cracking

The American Association of State Highway and Transportation Officials' *AASHTO LRFD Bridge Design Specifications*³ and state-of-the-art research for end zone design say that end zone reinforcement should resist at least 4% of the total prestressing force at transfer and the stress in the reinforcing bars should be 20 ksi (140 MPa) or less. Article 5.10.10.1 of the *AASHTO LRFD specifications*³ also states that the reinforcement resisting the splitting force at the end zones should be placed at each girder end within a distance of one-fourth the height of the girder. These requirements sometimes result in excessive end zone reinforcement, especially in highly

prestressed girders, which can lead to constructibility issues. Several DOTs have done research to determine design details that minimize end zone cracks. These studies have found that increasing the vertical reinforcement in the end zone does not always fully eliminate end zone cracking; rather, it can lead to congestion, which may have serious consequences for the service life and durability of the girder. To completely eliminate concrete cracks, the tensile capacity of the concrete must be increased significantly at the prestressed concrete girder end zone.

Ultra-high-performance concrete (UHPC) is an advanced cementitious material containing steel fibers and no coarse aggregate with compressive strengths greater than 22 ksi (150 MPa). Tensile strengths of steam-cured UHPC range from 1.2 to 1.7 ksi (8.3 to 11.7 MPa).⁴ As part of the Federal Highway Administration's research on UHPC, extensive material property tests have been performed to determine the strength, durability, and long-term stability of the material.⁵ The research showed very high concrete compressive strengths of 28.9 ksi (199 MPa) for UHPC thermally treated at 195°F (90.6°C) for 48 hours immediately following demolding, as specified by the manufacturer. The modulus of elasticity of the thermally treated UHPC was 7600 ksi (52.4 GPa). In the past decade, UHPC has been successfully implemented in the United States in precast concrete girders (I- and π -shaped girders⁶), precast concrete waffle decks,⁷ precast UHPC piles,⁸ and deck connections.⁹

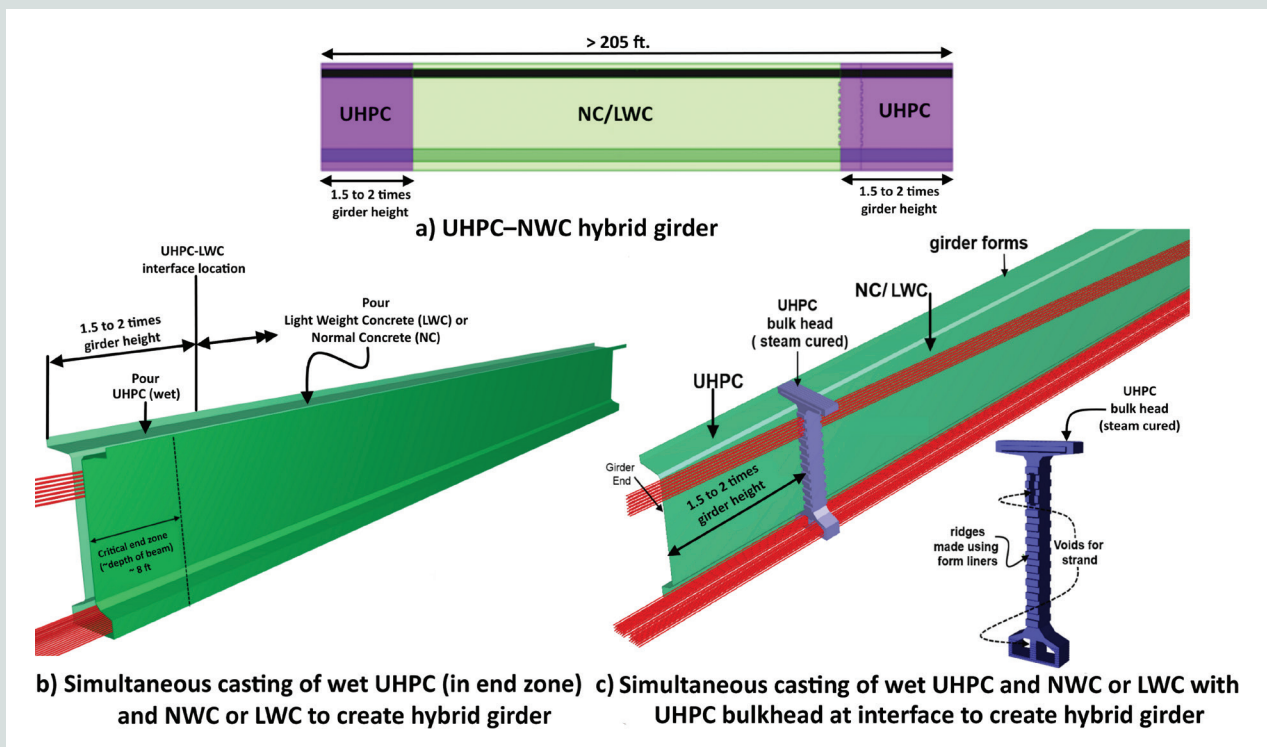


Figure 1. Long-span UHPC-NWC hybrid girder concept and possible casting methods. Note: LWC = lightweight concrete; NC = NWC = normalweight concrete; UHPC = ultra-high-performance concrete. 1 ft = 0.305 m.

UHPC is one of the only options currently available to create bridges with 100-year life spans and to provide an alternative to replace steel bridge girders with concrete girders of approximately equivalent capacity, depth, and weight. Highly optimized beam cross sections have been created for use with UHPC (π -shaped girder⁶), but their construction requires sophisticated formwork that is both expensive to manufacture and more difficult to use than formwork for traditional I-shaped girders. Full-length girders with UHPC would require new and more structurally efficient shapes that take advantage of the higher compressive and tensile strengths of UHPC and also minimize the increase in production costs. This is because commercial UHPC is generally 10 to 20 times the cost of standard high-performance concrete. This paper addresses these challenges with a hybrid girder concept that combines UHPC and normalweight concrete (NWC). The experimental and analytical research presented in this paper shows the improved performance of the hybrid girder.

Hybrid girder concept

The hybrid girder concept was developed as a cost-effective method to use UHPC in discrete critical locations to achieve longer-spanning prestressed girders using existing formwork shapes. The hybrid girder uses UHPC in the end zones over a distance equal to two times the depth of the girder and NWC for the rest of the girder (**Fig. 1**). Using UHPC in the anchorage zones takes advantage of the enhanced compressive (more than 22 ksi [150 MPa]) and tensile (more than 1.2 ksi [8.3 MPa]) capacity of UHPC to eliminate end zone cracking during prestress transfer. The benefits of this concept include the following:

- less end zone reinforcement, which improves constructibility
- the ability to use more strands in a standard cross section, which may mean that the strands do not require debonding or draping to reduce end zone stresses, leading to more efficient casting and potentially increasing the load-carrying capacity of the girders or allowing for fewer girder lines where end stresses limit the design
- a girder section with increased lateral stability, which is due to the increased tensile capacity of the UHPC section compared with NWC, that is capable of handling stresses when lifting devices are inset far from the ends of the girder
- shallower concrete members capable of spanning longer lengths compared with NWC, thus reducing impacts to hydrology or fill quantities or both
- an improved option for segmental construction where UHPC may be used in pier segments or anchorage zones for spliced post-tensioned girders with NWC or lightweight concrete (LWC) drop-in segments or main span products, improving the efficiency of the overall system and limiting the cost increase of using UHPC

Two casting concepts were developed for the pretensioned hybrid girder. The first concept requires coordination for placing UHPC in the end regions and NWC in the rest of the girder main span (**Fig. 1**). An overlap in the concrete placement of the girder sections will result where UHPC will be integrated with a stiffer NWC at the interface, thus creating a monolithic UHPC–NWC end region prior to detensioning. This concept appears complex and requires a coordinated effort during concrete placement to ensure that the interface is placed at the correct location.

The second casting concept minimizes the precision required for concrete placement by using a precast UHPC bulkhead with shear keys and blockouts for strands placed at a set distance from the girder ends (**Fig. 1**). NWC or LWC is placed between the UHPC bulkheads, and UHPC is placed at the girder ends. This concept creates two joints: one UHPC to UHPC and the other UHPC to LWC or NWC. The entire composite hybrid girder will be steam cured for 16 to 24 hours before prestress release, which will aid in strengthening the UHPC to 15 ksi (103 MPa) or greater and reduce long-term shrinkage.

Investigative approach

The hybrid girder concept focuses on using existing shapes and design procedures to extend prestressed concrete girder spans beyond 200 ft (61 m) with an average girder spacing of 8 to 10 ft (2.4 to 3.0 m). The structural response and behavior of hybrid girders will be critically affected by the interface performance under different loading conditions. Therefore, it is essential to understand and predict the end-region behavior, including critical stresses, crack formation in deep girders, and UHPC-to-conventional concrete interface shear and rupture behavior. **Figure 2** shows the integrated experimental and analytical approach used to validate the feasibility and structural performance of the hybrid girder. This paper presents the details of the experimental testing performed to understand the UHPC-to-NWC interface behavior. The experimental testing was followed by analysis of end-zone and shear behavior of 78 in. (1980 mm) deep bulb-tee (BT-78) prestressed concrete girders. Next, three-dimensional (3-D) finite element analysis (FEA) models for the interface and deep girder behaviors were developed and calibrated using the experimental data. The calibrated models were further used to evaluate the performance of the full-scale hybrid girder under critical design loading conditions derived from the AASHTO LRFD specifications.³

UHPC-to-NWC interface behavior

Previous research

There are few studies available that investigate the effect of design parameters such as interface roughness, NWC strength, and amount of reinforcement across the interface on the UHPC-to-NWC interface shear capacity. Muñoz et al.¹⁰ investigated the interface bond strength between UHPC

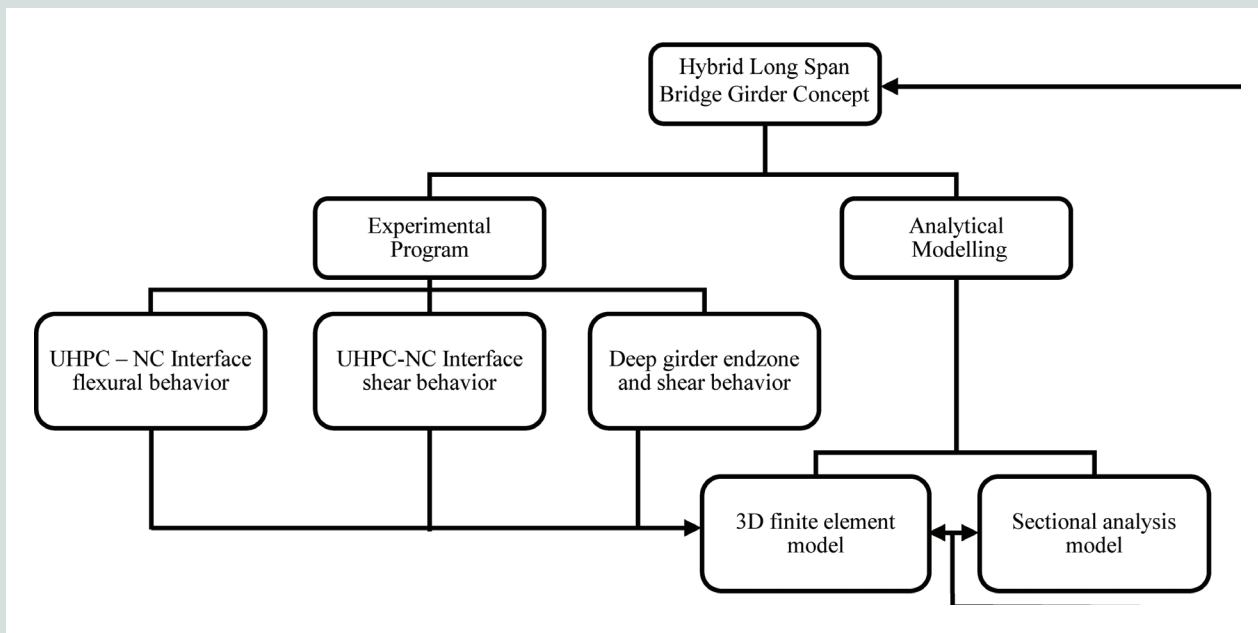


Figure 2. Investigative approach for long-span UHPC-NC hybrid girder concept. Note: 3D = three-dimensional; NC = normal-weight concrete; UHPC = ultra-high-performance concrete.

and NWC at eight days for four different degrees of interface roughness varying from 0.03 to 0.09 in. (0.76 to 2.3 mm). Aaleti and Sritharan¹¹ investigated the interface bond strength between UHPC and NWC for five different interface textures with roughness varying from 0.05 to 0.26 in. (1.3 to 6.6 mm) and three different concrete strengths. Both of these studies used the standard slant shear testing procedure (per ASTM C882¹²), and the test specimens contained no reinforcement across the interface. These studies showed that the interface shear capacity was greater than the NWC shear capacity. Crane¹³ and Jang et al.¹⁴ performed push-off tests on UHPC-NWC composite specimens with interface groove depths of 0.24 and 0.4 in. (6.1 and 10 mm), respectively. The specimens in these studies were not subjected to any external normal forces across the interface. Some of the specimens had no reinforcement passing across the interface, but a few of the specimens had reinforcement across the joint. These studies found that interface shear capacities of 0.53 and 0.55 ksi (3.7 and 3.8 MPa) can be achieved with 0.24 and 0.4 in. deep groove interface textures. These capacities were achieved with no application of normal force and no reinforcement passing across the interface.

There is limited research available on the tensile rupture behavior of the UHPC-to-NWC interface. Muñoz et al.¹⁰ performed splitting tensile tests (per ASTM C496¹⁵) and pull-off tests (per ASTM C1583¹⁶) on small prismatic composite specimens made of UHPC and NWC, which can be used as an indirect measure of UHPC-to-NWC interface behavior under pure bending. The tests investigated the effect of five different interface textures—smooth, chipped, brushed, sandblasted, and grooved—on the rupture strength of the speci-

mens and found that the splitting tensile capacity varied from 0.54 to 0.7 ksi (3.7 to 4.8 MPa) with texture roughness. The maximum value observed was for a grooved texture. These splitting-tension-capacity values were higher than the capacity of monolithically cast NWC specimens. Hussein et al.¹⁷ performed pull-off tests in accordance with ASTM C1404¹⁸ on UHPC-NWC composite specimens with an exposed aggregate surface finish for the interface. An average tensile stress value of 0.82 ksi (5.7 MPa) was measured in this study. The results of all these previous studies indicate that the UHPC-NWC composite system with sufficient surface preparation has a tensile capacity in the same range as an NWC monolithic system.

Even though the previous studies indicate sufficient shear capacity for the UHPC-to-NWC interface, none of the studies fully defined the load compared with the slip behavior along the length of the interface. In order to understand the performance of the hybrid girder and develop 3-D FEA models, it is critical to precisely define the interface behavior in terms of slip, dilation, crack opening, and strain development in the reinforcement crossing the interface.

Experimental program

Push-off tests

Small-scale push-off tests were performed on UHPC-NWC composite specimens with a 0.2 in. (5 mm) groove texture (Fig. 3). The composite specimens consisted of a 9 × 8.5 in. (229 × 216 mm) rectangular NWC block in interface with a 7 × 5.5 in. (178 × 140 mm) rectangular UHPC block. The

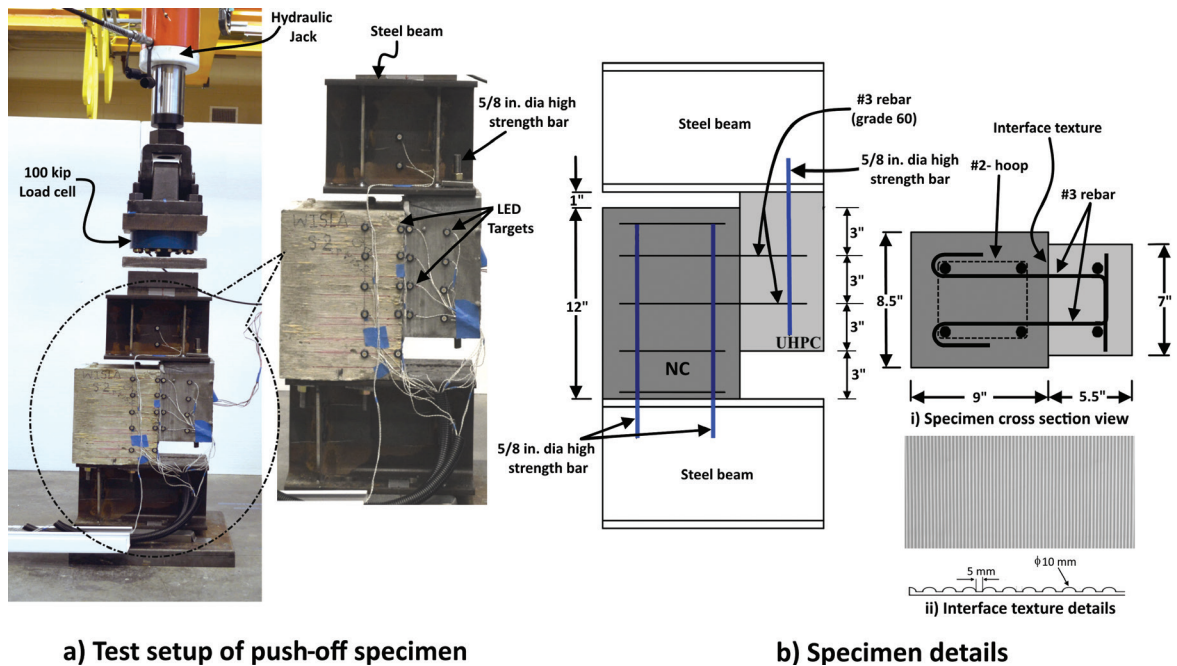


Figure 3. Push-off test setup and specimen details. Note: LED = light-emitting diode; NC = normalweight concrete; UHPC = ultra-high-performance concrete. #2 = no. 2 = 6M; #3 = no. 3 = 10M; 1" = 1 in. = 25.4 mm; 1 kip = 4.448 kN.

NWC block was proportioned to be slightly larger than the UHPC block and provided with no. 2 (6M) closed shear stirrups to prevent premature shear failure of the NWC block. To simplify the test setup, 0.625 in. (15.9 mm) diameter high-strength threaded steel rods were used as longitudinal reinforcement. The rods allowed the steel beams to be attached to the composite specimens and apply loading in line with the interface (Fig. 3). The NWC portion of the composite specimen was cast first with a standard 5 ksi (34 MPa) concrete, using a formliner to create the grooved interface texture. The formliner was used to create consistency in the interface texture between samples. Seven days after the NWC block was cast, the UHPC portion was cast using a commercially available UHPC that is produced by Lafarge North America. Figure 3 shows the typical dimensions and texture details of the specimens. In this figure, for specimen

SP-R0, the no. 3 reinforcement shown will not be present, for specimen SP-R2 only the bottom layer of the no. 3 reinforcement is provided, and for SP-R4 all of the reinforcement shown in the figure is provided.

A total of three specimens with a constant interface area and varying amounts of reinforcement across the interface were tested to failure. The amount of reinforcement was varied from no reinforcement to four no. 3 (10M) reinforcing bars across the interface (Table 1). The measured NWC and UHPC compressive strengths on the day of the test were 6.5 and 21 ksi (45 and 145 MPa), respectively. The specimen was subjected to shear loading using a hydraulic jack (Fig. 3). The test specimens were instrumented with load cells and a surface 3-D displacement measurement system to measure the applied loading and interface slip, respectively. The reinforce-

Table 1. UHPC-NWC push-off test specimen details and measured capacities

Specimen name	Reinforcement area across interface, in. ²	Interface area, in. ²	Peak load, kip	Shear stress, ksi	Slip at peak load, in.
SP-R0	0.00	63.68	30.94	0.49	0.010
SP-R2	0.22	61.43	38.14	0.62	0.010
SP-R4	0.44	62.81	60.55	0.96	0.017

Note: NWC = normalweight concrete; UHPC = ultra-high-performance concrete. 1 in. = 25.4 mm; 1 in.² = 645.2 mm²; 1 kip = 4.448 kN; 1 ksi = 6.895 MPa.

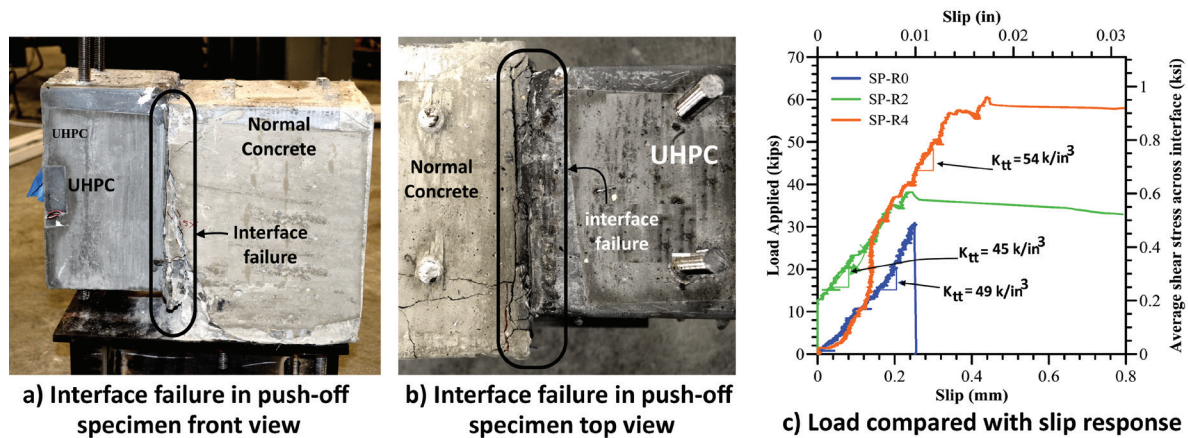
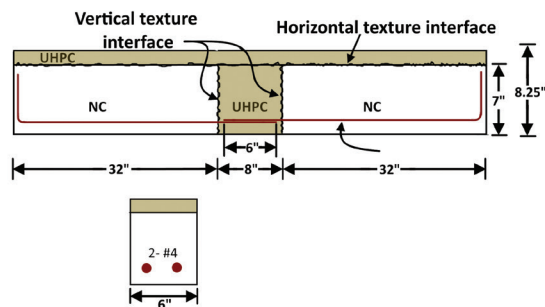


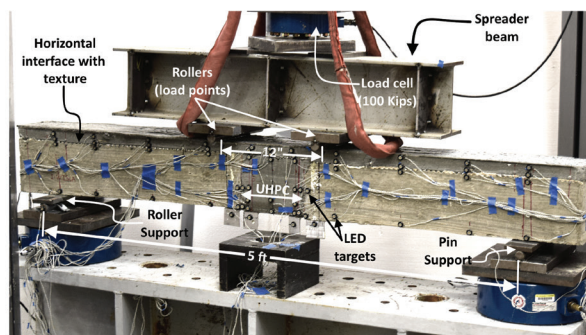
Figure 4. Push-off specimen failure and measured load compared with the slip responses. Note: K_{tt} = shear stiffness; UHPC = ultra-high-performance concrete. 1 kip = 4.448 kN; 1 ksi = 6.895 MPa; 1 kip/in.³ = 0.271 N/mm³.

ment across the interface was instrumented with strain gauges to monitor the engagement and contribution of the reinforcing bars to interface strength. All three specimens failed along the interface, with interface failure occurring on the NWC block side (Fig. 4). The slip along the interface was measured using the light-emitting diode (LED) targets of the surface 3-D displacement measurement system, and Fig. 4 shows the measured load compared with the slip response of each test specimen. Table 1 presents a summary of the push-off test results. The maximum average shear stress measured along the interface for the specimen without reinforcing bars was 0.49 ksi (3.4 MPa). This value is similar to the interface shear strengths of 0.53 and 0.55 ksi (3.7 and 3.8 MPa) measured in research studies by Crane¹³ and Jang et al.,¹⁴ respectively.

Thus, the experimental value of 0.49 ksi was taken as the cohesive strength of the interface for FEA modeling. Figure 4 shows that for specimens SP-R2 and SP-R4, an increase in load-carrying capacity was observed from 0 to 12 kip (0 to 53 kN) and 10 to 28 kip (44 to 125 kN), respectively, without any increase in slip. This can be attributed to a mechanical interlock aided by the presence of the reinforcing bars that are engaged before the surface interface cohesion capacity was reached. In specimens SP-R2 and SP-R4, higher shear capacities of 0.62 and 0.96 ksi (4.3 and 6.6 MPa) were obtained due to the additional contribution of the two no. 3 (10M) reinforcing bars in SP-R2 and four no. 3 reinforcing bars in SP-R4 across the interface. The measured average shear stiffness parameter K_{tt} of the interface was 49.33 kip/in.³ (13.39 N/mm³).



a) Details of UHPC-NWC composite beam



b) Test setup and instrumentation

Figure 5. Flexural testing specimen details and test setup. Note: LED = light-emitting diode; NC = NWC = normal weight concrete; UHPC = ultra-high-performance concrete. #4 = no. 4 = 13M; 1" = 1 in. = 25.4 mm; 1 ft = 0.305 m; 1 kip = 4.448 kN.

Flexural testing of UHPC-to-NWC interface

Four small-scale UHPC–NWC hybrid beam specimens were tested to failure under flexural loading to define the interface rupture behavior. The composite beam specimens consisted of two 32 in. (810 mm) long rectangular NWC beam segments connected using UHPC (Fig. 5). The NWC segments had a surface texture along the length of the top face and along the vertical face at one end. The vertical face had the same deep grooved texture as was used for the push-off specimens. The hybrid beam specimens were 6 in. (150 mm) wide, 8.25 in. (210 mm) deep, and 6 ft (1.83 m) long. All of the specimens had two no. 4 (13M) reinforcing bars for longitudinal reinforcement and no shear reinforcement.

The specimens were constructed by first casting the NWC segments with a formliner placed against the interface region. Next, after the NWC segments had gained strength for 28 days, the UHPC block was placed. The no. 4 (13M) longitudinal reinforcing bars were spliced for a length of 6 in. (150 mm) in the UHPC block. A layer of UHPC was also cast on top of the beam to increase its capacity and enable higher loads across the interface. Future studies are intended to investigate the viability of this method of casting to construct more efficient deck bulb-tee girders using UHPC and conventional concrete. All four specimens were tested using a four-point bending test setup (Fig. 5) to keep the vertical UHPC–NWC interface in a constant moment region. The loading was applied using a hydraulic jack under load control. The measured compressive strengths for NWC and UHPC on the day of testing were 6.53 and 21 ksi (45 and 145 MPa), respectively.

The specimens were extensively instrumented with LED targets and string potentiometers to capture local deformations across the interfaces and global displacements of the beam. The average strains in the constant moment region were measured at seven locations along the height of the beam using LED pairs (Fig. 5). The crack opening across the interface, average strains along the height of the specimens, and neutral axis depth were also obtained from the LED targets. The measured bending moment value at the initiation of cracking was used along with the transformed section properties and the experimentally obtained neutral axis depth to calculate the rupture strength of the interface. The calculated rupture strength values for the test specimens are presented in Table 2.

End zone cracking and shear testing of BT-78 girders

As part of a research project supported by the Alabama DOT, the effectiveness of various types of reinforcement detailing on mitigating the end zone cracking and its impact on girder shear behavior was evaluated using a BT-78 girder. The girder specimen was reinforced with sixty-six 0.6 in. (15.2 mm) diameter prestressing strands (Fig. 6) and was constructed

Table 2. UHPC-to-NWC interface flexural testing results

Specimen name	Cracking load, kip	Rupture strength, ksi	Failure load, kip
Beam 1	2.2	0.45	12.68
Beam 2	2.6	0.44	13.34
Beam 3	2.2	0.46	12.76
Beam 4	1.9	0.39	11.36

Note: NWC = normalweight concrete; UHPC = ultra-high-performance concrete. 1 kip = 4.448 kN; 1 ksi = 6.895 MPa.

using 10 ksi (69 MPa) self-consolidating concrete. A total of four 54 ft (16.5 m) long BT-78 girder specimens representing the 54 ft end segment of a 180 ft (54.9 m) long girder were cast with different end zone reinforcement details. All of the test specimens were extensively instrumented with concrete and steel strain gauges to capture critical strains in the end zone during detensioning. Figure 6 shows the observed end zone cracking in one of the specimens. More details about the experimental field testing can be found in Ronanki et al.¹⁹ The results from this study obtained at release were used in this paper to check the adequacy of the FEA models in capturing the behavior of deep prestressed concrete girders.

All four specimens were tested at the Large Scale Structures Laboratory at the University of Alabama in Tuscaloosa using a three-point loading test setup (Fig. 6). All of the test specimens were subjected to loads on the order of 800 kip (3560 kN) that were designed to cause significant shear cracking. More details about testing and results can be found in Burkhalter.²⁰ Figure 6 also shows the web shear cracking experienced by all of the tests specimens prior to reaching the peak load and the measured force compared with the displacement response for each specimen.

Calibration of FEA models

The FEA models used in this study were performed in ATENA version 5 software and used nonlinear material behavior for all elements and material types (that is, NWC, reinforcing steel, and UHPC). The specimen geometries were built largely using eight-node brick elements. For the cases where the geometry could not be defined using a brick element, six-node wedge elements were used. The wedge elements were chosen because they offer a higher degree of accuracy for the results than tetrahedral elements. In all of the FEA models in this study, the application of prestress was performed through the prestressing load module in the FEA software. Further, the interaction between any mild-steel reinforcement and NWC or UHPC was modeled using a bond stress-slip model. The parameters needed for the bond stress-slip models were adopted from the Euro-International Concrete Committee and International Federation for Prestressing's *CEB-FIP Model Code 1990: Design Code* (CEB-FIP code).²¹

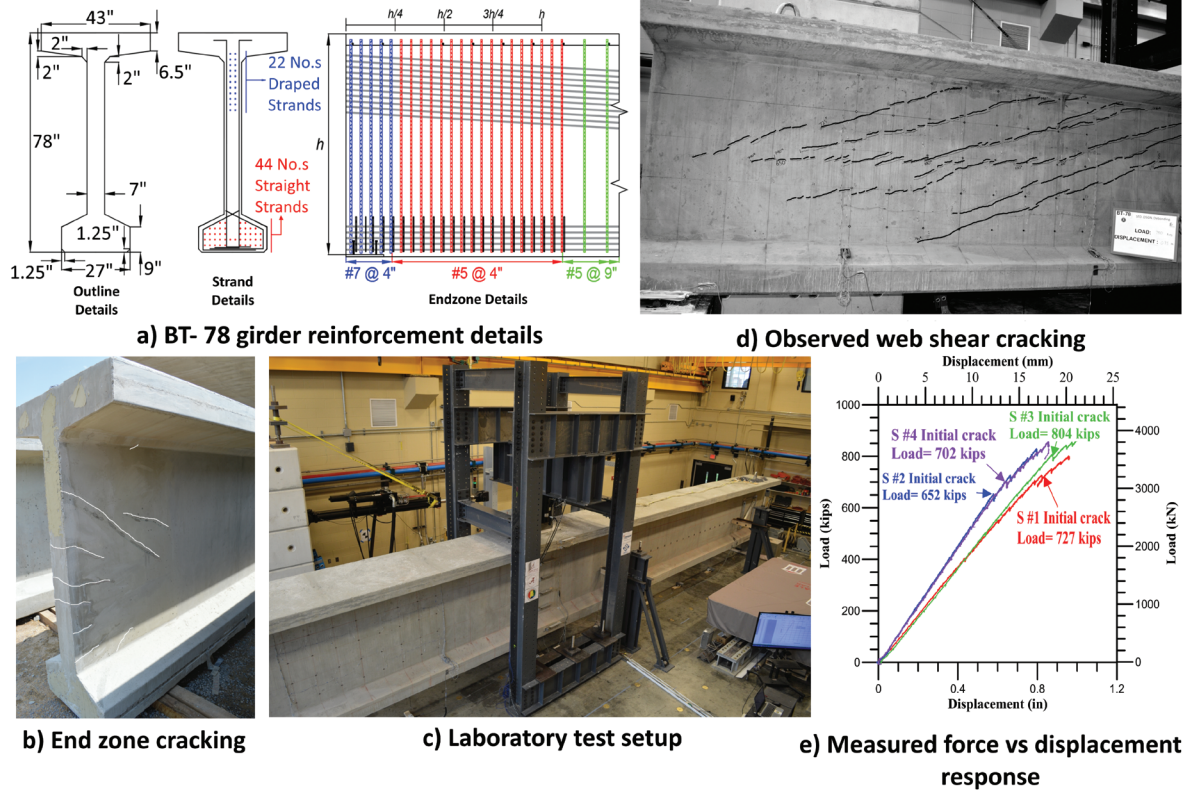


Figure 6. Details of BT-78 girder field end zone monitoring and laboratory shear testing. Note: BT-78 = 78 in. deep bulb-tee girder; h = girder height. #5 = no. 5 = 16M; #7 = no. 7 = 22M; 1" = 1 in. = 25.4 mm.

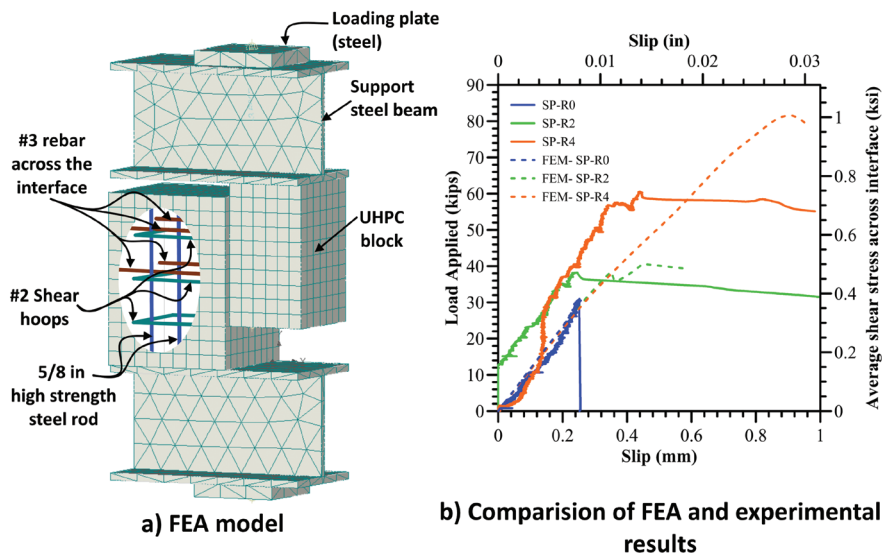


Figure 7. FEA model and comparison of experimental and FEA results for push-off specimens. Note: FEA = finite element analysis; SP-R0 = push-off test specimen with no reinforcement across the interface; SP-R2 = push-off test specimen with two reinforcing bars across the interface; SP-R4 = push-off test specimen with four reinforcing bars across the interface; UHPC = ultra-high-performance concrete. #2 = no. 2 = 6M; #3 = no. 3 = 10M; 1 in. = 25.4 mm; 1 kip = 4.448 kN; 1 ksi = 6.895 MPa.

Table 3. UHPC and NWC modeling parameters and properties

	Material parameters		
	Interface specimen concrete	Hybrid girder concrete	UHPC
Compressive strength, psi	6500	9000	21,000
Modulus of elasticity, ksi	4595	5407	7590
Poisson's ratio	0.2	0.2	0.2
Modulus of rupture, psi	604	711	1200*

Note: Interface parameters for 0.2 UHPC-to-NWC texture were $C = 0.52$ ksi, $f_t = 0.43$ ksi, $K_{nn} = 7905$ kip/in.³, $K_{tt} = 49$ kip/in.³, $\mu = 0.4$. C = cohesive strength; f_t = tensile strength; K_{nn} = tensile stiffness; K_{tt} = shear stiffness; NWC = normalweight concrete; UHPC = ultra-high-performance concrete; μ = coefficient of friction. 1 in = 25.4 mm; 1 kip = 4.445 kN; 1 psi = 6.895 kPa; 1 ksi = 6.895 MPa; 1 kip/in.³ = 0.271 N/mm³.

* Postcracking sustained load behavior was also modeled at a peak f_t of 1600 psi.

Modeling of UHPC-to-NWC interface behavior

The interaction between the UHPC and NWC at the interface was modeled using a constitutive contact model called the *interface material model* in the FEA software. The behavior of this contact model is defined by shear stiffness, tensile stiffness, cohesion strength, tensile strength, and coefficient of friction. These parameters were chosen based on the experimental work discussed previously in this paper. The values of shear stiffness K_{tt} and cohesive strength C were obtained from the push-off tests. The values of tensile stiffness K_{nn} and tensile strength f_t were obtained from the UHPC–NWC composite beam tests. The value for the coefficient of friction μ was taken from the study conducted by Aaleti and Sritharan,¹¹ which used slant shear specimens to obtain the effect of normal force on the enhancement of shear strength.

Both the push-off tests and composite beam tests were modeled in the FEA software, and the analytical results were compared with measured experimental values to examine the degree of accuracy in using the chosen parameters to capture the interface behavior. For all of the test specimens, the NWC properties, such as Young's modulus and modulus of rupture, were calculated using equations from the American Concrete Institute's (ACI's) *Building Code Requirements for Structural Concrete (ACI 318-14) and Commentary (ACI 318R-14)*.²² The stress-strain behavior of the UHPC was modeled using a user-defined cementitious material model representing the material behavior proposed by Graybeal⁵ and Sritharan et al.⁴ **Table 3** summarizes the critical material and interface model parameters used in the FEA and calibration of test specimens.

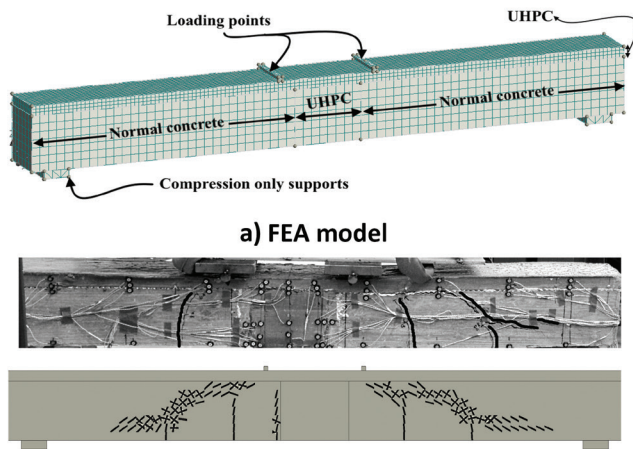
Push-off specimen The push-off specimen FEA models were developed using eight-node linear brick elements for NWC and UHPC sections. The shear stirrups in the NWC block, the reinforcing bars crossing the interface, and the high-strength threaded steel rods were modeled using truss elements. **Figure 7** shows the FEA model of the push-off test specimen and the force compared with the slip response for the experimental tests and the FEA. **Figure 7** also shows that the behavior of the specimen with no reinforcement across the

interface, SP-R0, was accurately captured using the assumed interface properties. However, for the specimen with two reinforcing bars across the interface, SP-R2, although the peak load values were accurately predicted, the slip at first occurrence of peak load was overestimated by the FEA.

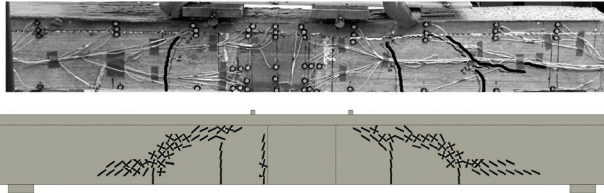
In specimen SP-R4, which has four reinforcing bars passing across the interface at two distinct levels, the FEA model simulation follows a trend similar to that of the model for SP-R2 but overpredicts the failure load and the slip at first occurrence of peak load. This inaccuracy may be caused by using truss elements to model reinforcing bars, which will not simulate the bars' bending stiffness. A further refinement of this simulation would be to model the reinforcing bars using 3-D solid elements with an appropriate contact behavior between the reinforcing bar surface and concrete. Such an analysis would require further investigation into the contact mechanics between the reinforcing bar surface and concrete, which is beyond the scope of this paper. However, the experimental results indicate a sustained peak load for large slip values, leading to an eventual failure, which was effectively captured in the FEA simulations.

Composite beam specimen The FEA model for composite beams was also built using eight-node linear brick elements with reinforcing bars modeled as truss elements (**Fig. 8**). **Figure 8** shows the experimental and analytical load compared with the midspan displacement response and the damage patterns for one of the specimens. **Figure 8** also shows that the FEA results were accurate in predicting the beam behavior prior to the rupture of the interface.

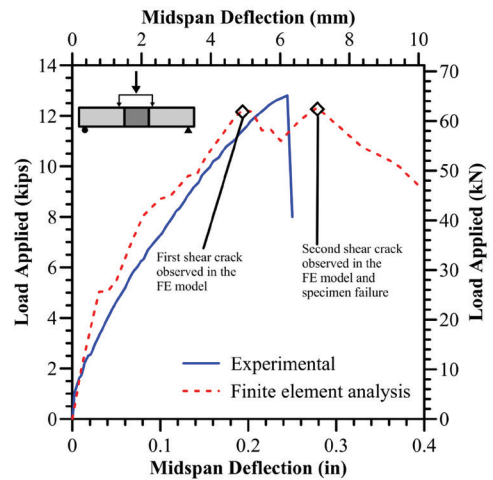
After the interface separates, the FEA model predicted higher stiffness compared with the experimental response. This inaccuracy may be caused by using the normal stiffness behavior for the interface model, which follows a gradual tension softening rather than a sharp degradation. In the experimental specimens, once separation occurred between the two surfaces at the interface, the behavior was governed only by the stiffness of the reinforcing bar, whereas in the FEA model the interface normal displacements continue to deform according to the stiffness values used prior to separation.



a) FEA model



b) Comparison of experimental and FEA crack patterns



c) Force compared with displacement response

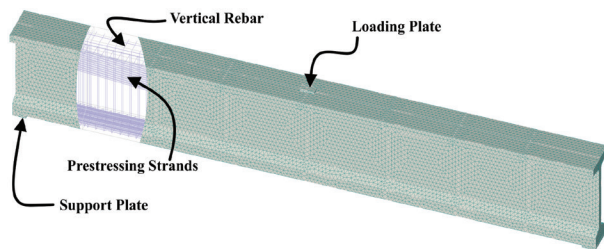
Figure 8. FEA model and comparison of experimental and FEA results for composite beam specimens. Note: FEA = finite element analysis; UHPC = ultra-high-performance concrete.

This limitation of the FEA leads to underprediction of displacements only in the case where an interface separation is expected. For the proposed hybrid girder concept, the maximum tensile forces were designed not to exceed the rupture limit, and an interface separation was not expected. The FEA model accurately captured peak failure load and the corre-

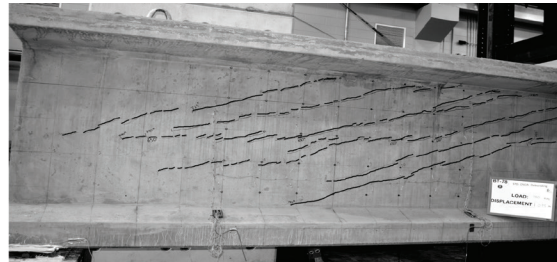
sponding damage to the specimen (Fig. 8).

Modeling of deep bulb-tee prestressed concrete girders

The FEA model for the bulb-tee girder was built using linear



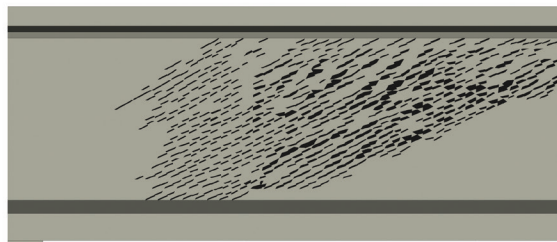
a) FEA meshing and model details



c) Observed web shear cracking after lab testing



b) Comparison of observed and FEA cracking after detensioning



d) Results of cracking from FEA simulation of lab tests

Figure 9. FEA model and comparison of experimental and FEA results for BT-78 girder specimens. Note: BT-78 = 78 in. (1980 mm) deep bulb-tee girder; FEA = finite element analysis.

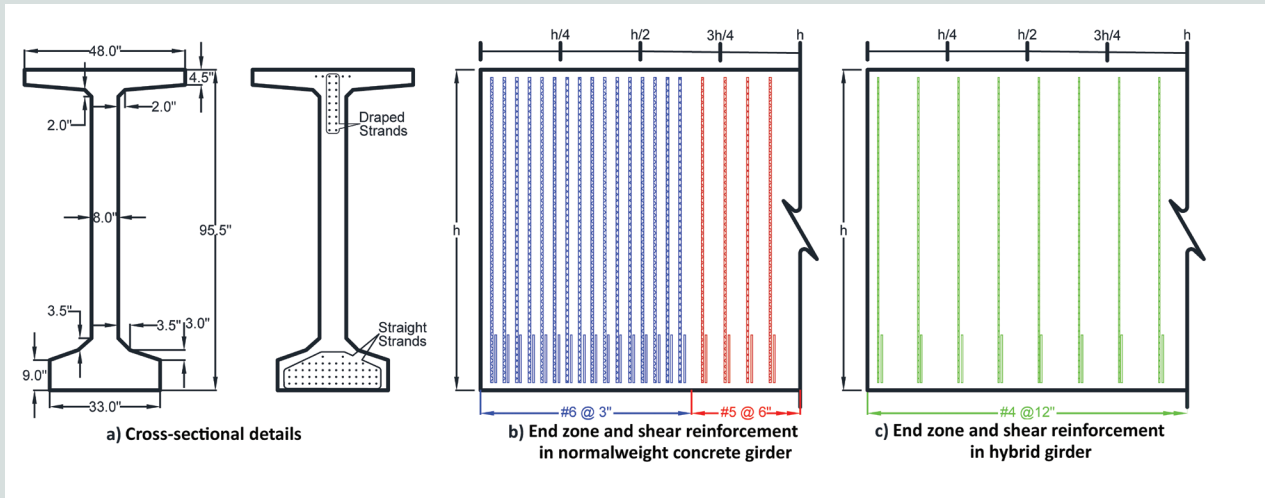


Figure 10. Cross section and reinforcement details of normalweight and hybrid PCEF girder. Note: h = girder height; PCEF = Precast Concrete Economical Fabrication Committee standard bulb-tee girder shape. #4 = no. 4 = 13M; #5 = no. 5 = 16M; #6 = no. 6 = 19M. 1" = 1 in. = 25.4 mm.

tetrahedral elements with an element size of 4 in. (100 mm) (Fig. 9). A single FEA model was used to simulate the release of prestressing strands and the laboratory shear testing (Fig. 6) with appropriate measured concrete material properties. The measured average concrete compressive strengths for the girders at prestress release and at the time of laboratory testing were 9.3 and 11.8 ksi (64.1 and 81.4 MPa), respectively. The concrete material parameters used to model the girder detensioning behavior are presented in Table 3. Prestress was applied to the model using the prestressing load module in the FEA software. The interaction between reinforcement and NWC or UHPC was addressed using a bond stress-slip model with parameter values suggested in the CEB-FIP code.²⁰

Figure 9 compares the end zone cracking predicted by the FEA model with the field-observed cracking, which shows that the FEA model accurately predicted the end zone cracking in the specimen. Figure 9 also shows that the FEA model was able to accurately capture the expected damage in deep girders due to shear loading. The modeling approach in the software can effectively simulate the end zone and shear behavior in deep girders and can be used to evaluate the performance of the hybrid girder under different loading conditions.

Analytical investigation of hybrid girder behavior

Prototype design and simplified analysis

After the calibrated FEA modeling approach and necessary parameters were established, a baseline girder design for a 205 ft (62.5 m) long, simply supported NWC girder was developed using a Precast Concrete Economical Fabrication Committee standard bulb-tee (PCEF-95) girder shape to investigate the hybrid girder concept and compare its performance with that of a traditional concrete girder design.

The PCEF-95 girder shape offers the advantage of having enough cross-sectional area in the bottom bulb to accommodate additional prestressing strands. It has an 8 in. (200 mm) thick web that enables more-efficient shear transfer across the UHPC-to-NWC interface in a hybrid girder. The girder cross section was designed for 8 ft (2.4 m) girder spacing using 10 ksi (69 MPa) concrete and meeting the requirements of the AASHTO LRFD specifications.³

The service-level and strength-level shear demands for the PCEF-95 section for the assumed lane configuration were calculated as 408 and 528 kip (1815 and 2350 kN), respectively. The service-level and strength-level moment demands were calculated as 20,753 and 26,847 kip-ft (28,136 and 36,398 kN-m), respectively. This resulted in a girder section with a total of seventy-eight 0.6 in. (15.2 mm) diameter strands at the girder midspan. Figure 10 shows the cross-section details of the girder at midspan. A concrete strength of 6.8 ksi (46.9 MPa) was used for prestress release to meet the AASHTO LRFD specifications requirements for critical stresses at release.

The shear reinforcement and end zone reinforcement for the NWC girder was designed using the AASHTO LRFD specifications.³ Shear and end zone reinforcement included no. 6 (19M) stirrups (diameter of reinforcement $d_b = 0.75$ in. [19 mm]) with two legs and center-to-center spacing of 3, 6, or 12 in. (75, 150, or 300 mm), depending on the region along the length of the girder. The end zone reinforcement was designed to resist 4% of the total prestressing force and detailed per the AASHTO LRFD specifications³ requirements. Figure 10 shows the end zone and shear reinforcement details for the NWC girder.

The UHPC–NWC hybrid girder was designed with UHPC for a length of 15.92 ft (4.85 m) on both girder ends. In the hybrid girder, no. 4 (13M) stirrups ($d_b = 0.5$ in. [13 mm]) with

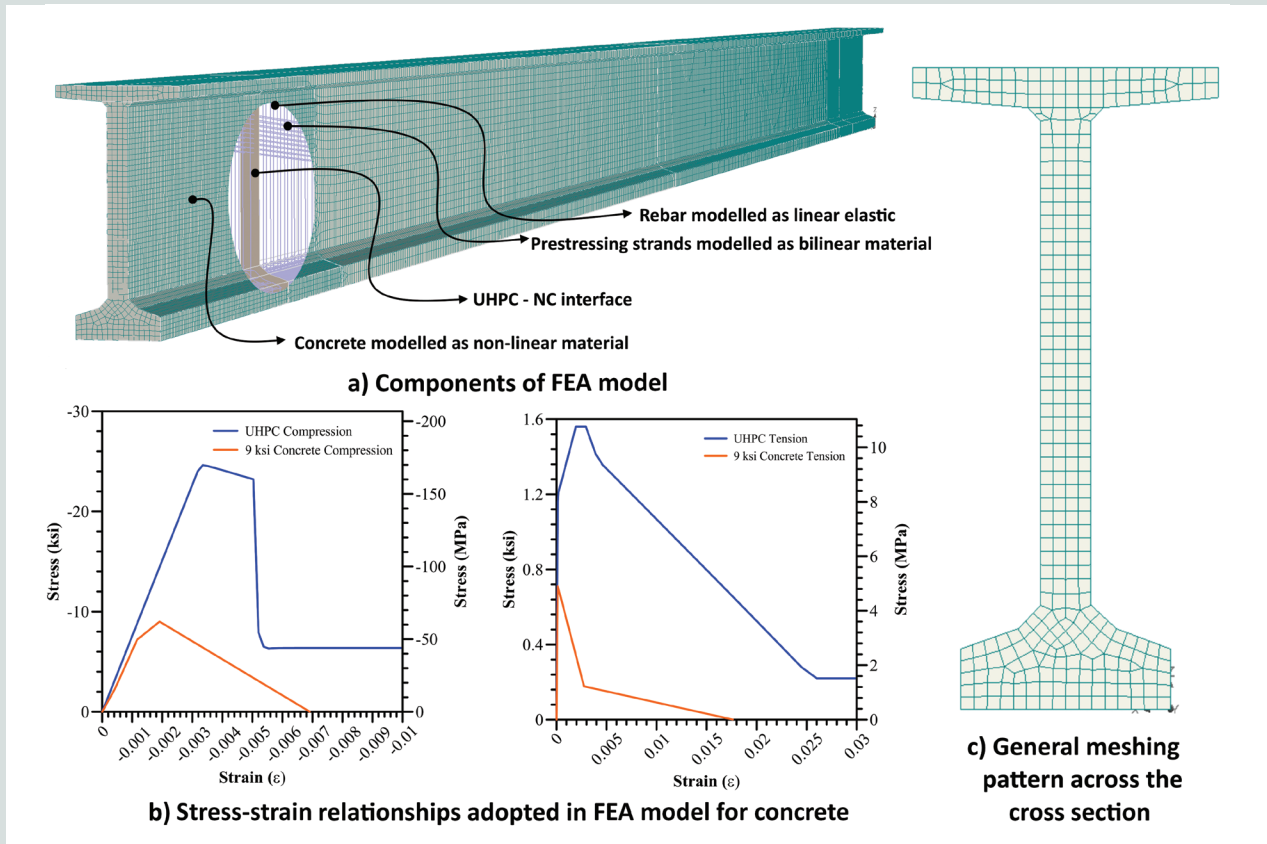


Figure 11. Hybrid girder FEA model details. Note: FEA = finite element analysis; NC = normalweight concrete; UHPC = ultra-high-performance concrete. 1 ksi = 6.895 MPa.

two legs and 12 in. spacing for the entire girder length were used as shear and end zone reinforcement (Fig. 10). The reinforcement design was done considering a conservative value for improved mechanical properties of the UHPC. The UHPC was assumed to have at least the same mechanical properties as the UHPC used in the experimental testing.

FEA modeling of hybrid girder

The feasibility of the hybrid girder was investigated using the validated FEA modeling techniques discussed previously. A full-scale 205 ft (62.5 m) long girder was modeled using the FEA software (Fig. 11). The model was divided into three zones representing various areas of interest (Fig. 11).

Zone 1 represents the region over a distance of two times the height of the girder from both ends, which consists of UHPC and was examined primarily for anchorage stresses, end zone cracking, and UHPC-to-NWC interface stresses. Zone 2 extends 95.5 in. (2430 mm) from the end of zone 1 toward the midspan on either end, consists of NWC, and was examined primarily for interface stresses. Zone 3 represents the remainder of the girder between the zone 2 regions on either end.

Nonlinear cementitious material models were used to model the NWC and UHPC elements, and a bilinear material model

was adopted for the prestressing strands. Because the reinforcing bar stresses were expected to remain within the elastic limits, they were modeled as linear elastic materials. Figure 11 shows the stress-strain relationships that were used in the FEA for concrete materials.

Meshing in zones 1 and 2 used a typical element size of 2 in. (50 mm). Zone 3 was meshed using a typical element size of 4 in. (100 mm). Figure 11 also shows the general meshing pattern across the cross section. The behavior and performance of the hybrid girder under different loading conditions, including detensioning, maximum moment, and maximum shear load cases, were evaluated using the aforementioned FEA model.

The hybrid girder was assumed to be simply supported for all loading conditions. The girder was analyzed in stages to mimic the expected construction sequence, and the corresponding loading was applied in three phases. First, a stagewise prestressing load was applied to the girder along with the self-weight of the girder to mimic the detensioning at a precasting plant. This was followed by applying additional loading to the girder to account for the placement of an 8 in. (200 mm) thick cast-in-place concrete deck. Stagewise construction is modeled in the FEA software by adding new elements (structural members) to existing models after certain load cases, such as prestressing, are applied.

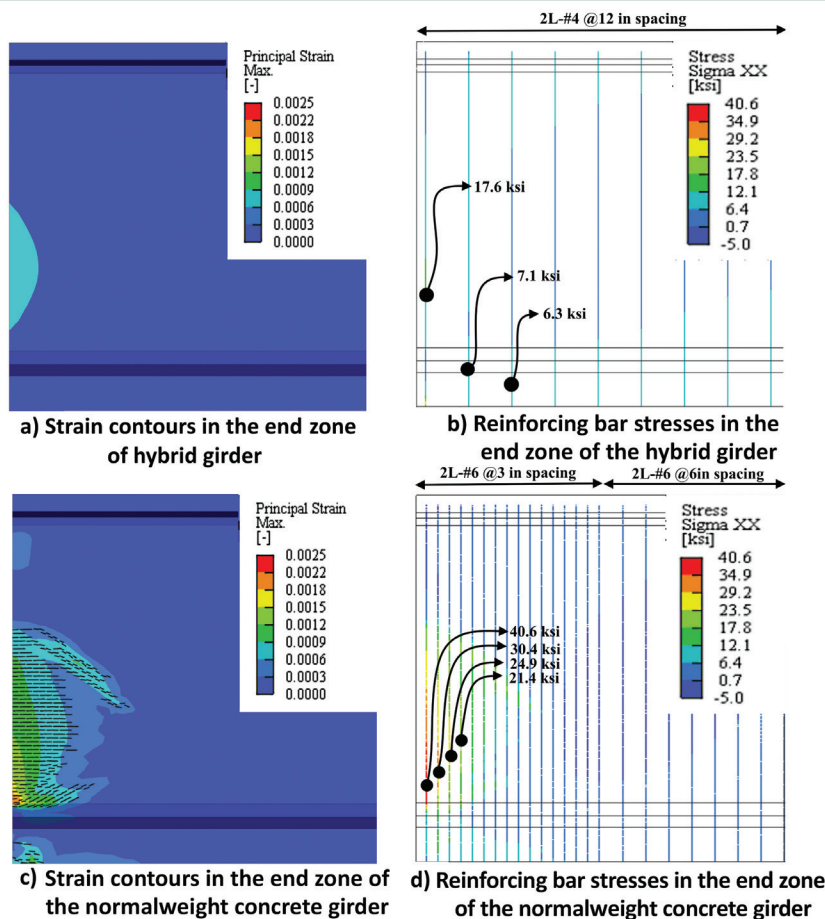


Figure 12. Hybrid girder FEA model details. Note: FEA = finite element analysis. #4 = no. 4 = 13M; #6 = no. 6 = 19M. 1 in. = 25.4 mm; 1 ksi = 6.895 MPa.

For the analysis of maximum moment and shear load cases, an 8 in. (200 mm) thick cast-in-place concrete deck was added to the top of the girder to simulate the composite girder and deck section that resists the design loads. The composite girder section was subjected to combined dead load plus live load corresponding to maximum moment and shear in the girder and UHPC-to-NWC interface. The live load applied to the girder corresponded to the HL-93 loading (design truck + 640 lb/ft [9.3 kN/m] lane load) as recommended in the AASHTO LRFD specifications.³

Results and discussion

End zone cracking at strand release

Principal strain contours of the concrete matrix and the vertical reinforcing bar stresses were examined to evaluate the performance of UHPC in the end zone. **Figure 12** presents a comparison of critical strains in the end zone region of the PCEF-95 girder with NWC and the PCEF-95 UHPC–NWC hybrid girder. **Figure 12** also shows that no cracking is expected in the end zone of the PCEF-95 hybrid girder during detensioning.

The strains across the cross section generally remain well within the cracking strain limit of UHPC. Strains above the cracking limit were observed in a small isolated area near the very end of the hybrid girder, activating the first reinforcing bar close to the girder end.

The stress in the first reinforcing bar was 17.6 ksi (121 MPa), which is less than the 20 ksi (140 MPa) (Fig. 12) recommended by the AASHTO LRFD specifications.

The low reinforcing bar stress indicates that the cracks formed (if any) would be very fine and would not have any impact on structural performance. **Figure 12** shows the end zone strains in the NWC girder. The figure shows that considerable cracking is expected in the end zone of a PCEF-95 girder with NWC.

The bar stresses in the NWC girder exceed the AASHTO LRFD specifications limit of 20 ksi (Fig. 12). The superior performance in the end zone shown by the hybrid girder can be attributed to the splitting forces being resisted by a continuous UHPC matrix, compared with discrete reinforcing bar locations in the NWC.

Maximum moment and maximum shear load case

Figure 13 presents the distribution of the interface shear and normal stresses in the hybrid girder from the FEA performed for maximum moment and maximum shear load cases. Figure 13 also shows that the top and bottom stresses in the hybrid girder remain within the AASHTO LRFD specifications limits.

The maximum observed compressive stress in the girder was 3.9 ksi (27 MPa), which is equivalent to $0.43 f'_c$. There were no tensile stresses observed in the girder from the applied dead and live loads.

The stresses along the UHPC-to-NWC interface of the hybrid girder were also examined for both load cases. Figure 13 shows the shear stress demand on the interface from the worst-case shear load. The majority of the cross-sectional area along the interface experienced shear stresses less than 0.49 ksi (3.4 MPa), the interface shear capacity obtained for the push-off specimen with no interface reinforcement.

In the maximum moment load case, a maximum shear stress of 0.89 ksi (6.1 MPa) occurred at the location of the draped strands along the interface height. In the maximum shear force at the interface load case, the HL-93 truck loading was placed directly on top of the interface. Because a large portion of the forces acting on the girder were dead load and uniformly distributed lane load, the change of truck position did not cause significant changes to the stress contours compared with the maximum moment load case. The maximum shear stress occurred at the location of the draped strands along the interface height, and the value of the maximum shear stress increased to 0.91 ksi (6.3 MPa). The maximum shear stress demands across the interface were less than the interface shear capacity obtained for the push-off specimen with reinforcement (Table 1).

The presence of prestressing strands, the higher concrete strength for the girder (9 ksi [62 MPa] compared with 6.5 ksi [45 MPa] concrete used in push-off specimens), and the presence of normal forces on the interface further increased the shear capacity of the interface compared with the small-scale tests presented in this paper. The peak value of shear stress in the interface was observed at a distance of approximately

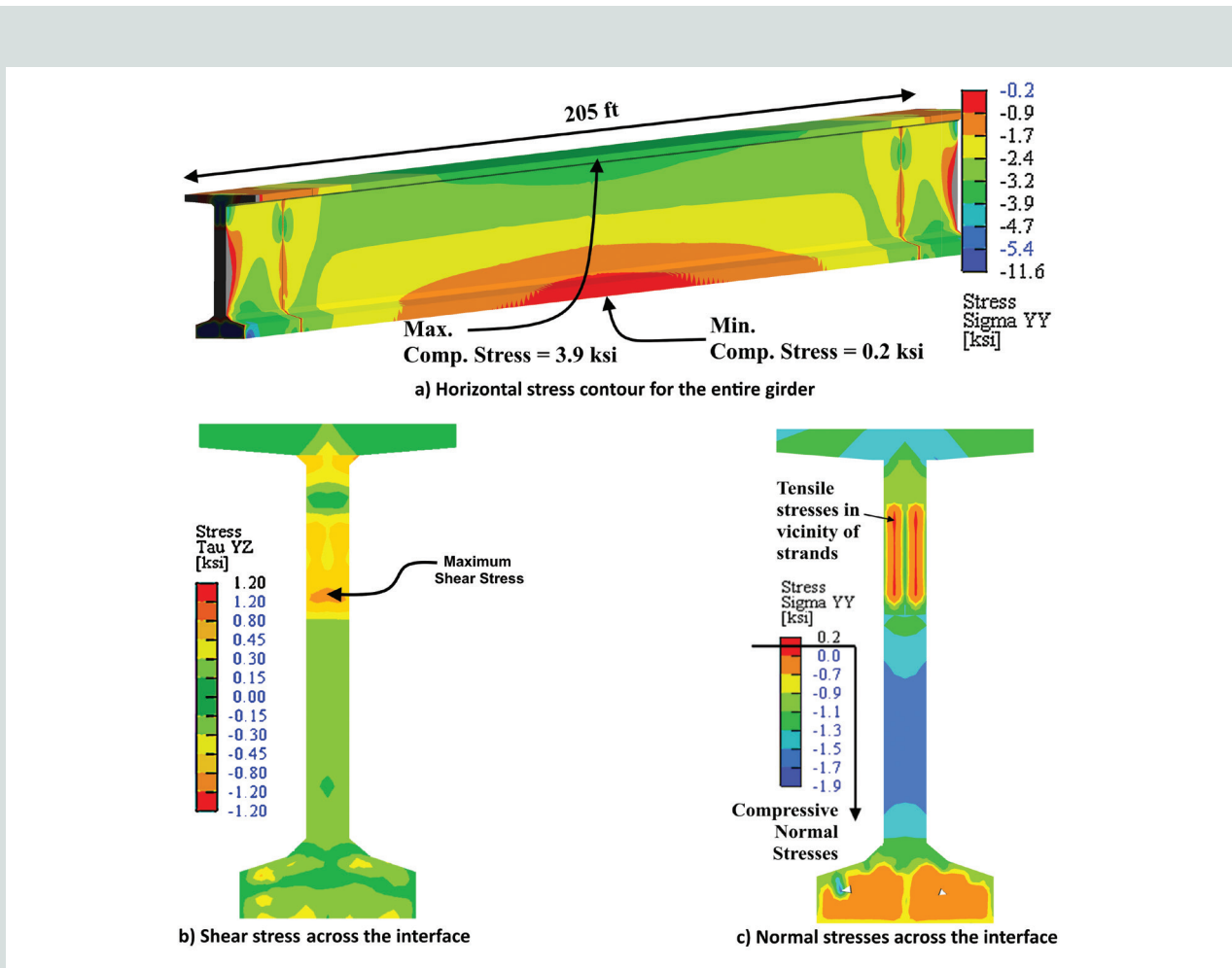


Figure 13. Critical stress distribution in the hybrid girder for maximum moment and maximum shear load cases. Note: Comp. = compressive; Max. = maximum; Min. = minimum. 1 ft = 0.305 m; 1 ksi = 6.895 MPa.

one-third the height of the girder measured from the top, and it decreased in magnitude farther away from this position.

Figure 13 shows the distribution of normal stresses across the UHPC-to-NWC interface along the height of the interface. Figure 13 also shows that the majority of the cross section at the interface location was under compression as expected. Tensile stresses less than 200 psi (1380 kPa) occurred over a very small area near the draped prestressing strands. This could be due to the bond stresses between the strands and surrounding concrete. These tensile stress values were well below the interface rupture strength of 0.43 ksi (3.0 MPa) obtained from beam tests.

Conclusion

This paper presents a long-span hybrid girder concept by introducing UHPC in critical regions of NWC girders. Experimental testing was conducted to define the UHPC-to-NWC interface behavior. FEA models for deep girders and UHPC-to-NWC interfaces were calibrated using the test results. The calibrated FEA models were used to investigate the performance of a full-scale hybrid girder. The following conclusions were reached based on the experimental and FEA study:

- The push-off specimen tests indicated that the 0.2 in. (5 mm) deep grooved-texture UHPC-to-NWC interface had sufficient shear capacity to carry the expected loads for a 205 ft (62.5 m) long girder. The measured shear strength across the UHPC-to-NWC interface varied from 0.49 to 0.96 ksi (3.4 to 6.6 MPa), depending on the amount of reinforcement across the interface. The shear strength increased with increased reinforcement area across the interface.
- The tensile strength for the 0.2 in. (5 mm) deep grooved-texture UHPC-to-NWC interface was found to be 0.44 ksi (3.0 MPa), which corresponds to a value of $5.2 \sqrt{f'_c}$ of the NWC. This value is lower than the modulus of rupture of NWC, indicating that the interface rupture strength should be used for performance evaluation or possible cracking in the hybrid girder.
- The FEA modeling approach and the interface parameters used in this study effectively captured the behavior of the interface for the case with no reinforcing bars across the interface. The failure load and slip values predicted by the model were within 95% of the experimentally measured values. Modeling reinforcing bars across the interface using a truss element did not fully capture the dowel action and stiffness of the interface. The failure loads calculated using the FEA models were within 5% of experimental values. However, the interface slip values were overpredicted by 30% for push-off specimen SP-R4.
- The FEA models for BT-78 girders accurately simulated the end zone cracking during detensioning and the web shear cracking in a BT-78 girder.

- The FEA of the hybrid girder supports the hypothesis that the hybrid girder concept can completely eliminate the end zone cracking problems in heavily prestressed girder shapes, such as PCEF 95. It will also drastically reduce the amount of end zone reinforcement required compared with girders designed with NWC. This will greatly reduce the congestion issues often observed when fabricating long-span girders. No end zone cracks were observed in the FEA of the 205 ft (62.5 m) long hybrid girder with a vertical reinforcing bar configuration of no. 4 (13M) reinforcing bars with two legs placed at 12 in. (300 mm) spacing.
- No interface separation was expected in the hybrid girder under HL-93 loading. The normal stresses and shear stresses at the interface were well below the measured capacities for the 0.2 in. (5 mm) deep grooved-texture UHPC-to-NWC interface. The hybrid girder details proposed in this paper can safely carry the expected loads of a 205 ft (62.5 m) long girder with 8 ft (2.4 m) girder spacing.

Acknowledgments

The authors would like to acknowledge and thank Lafarge North America for providing the UHPC material required to perform the small-scale testing presented in this study. The authors also would like to acknowledge the financial support provided by a Research Grants Council grant from the University of Alabama and the Alabama Transportation Institute. The assistance provided by Collin Sewell, structural lab manager at the University of Alabama, and several undergraduate and graduate students in specimen construction and testing is also greatly appreciated.

References

1. FHWA (Federal Highway Administration). "Tables of Frequently Requested NBI Information." Updated March 6, 2019. <https://www.fhwa.dot.gov/bridge/britab.cfm>.
2. Castrodale, Reid W., and Christopher D. White. 2004. "Extending Span Ranges of Precast Prestressed Concrete Girders." National Cooperative Highway Research Program report 517. Washington, DC: Transportation Research Board.
3. AASHTO (American Association of State Highway and Transportation Officials). 2015. *AASHTO LRFD Bridge Design Specifications*. 8th ed. Washington, DC: AASHTO.
4. Sritharan, S., B. Bristow, and V. Perry. 2003. "Characterizing an Ultra-High Performance Material for Bridge Applications under Extreme Loads." In *3rd International Symposium on High Performance Concrete, PCI National Bridge Conference Proceedings October 19–22, 2003, Orlando, FL*. Chicago, IL: PCI. CD-ROM.
5. Graybeal, Benjamin A. 2006. "Material Property Charac-

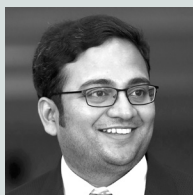
terization of Ultra-High Performance Concrete.” Report FHWA-HRT-06-103. McLean, VA: FHWA.

6. Graybeal, Benjamin A. 2009. “Structural Behavior of a 2nd Generation UHPC Pi-Girder.” Report FHWA-HRT-09-069. McLean, VA: FHWA.
7. Aaleti, Sriram R., Sri Sritharan, Dean Bierwagen, and Terry J. Wipf. 2011. “Structural Behavior of Waffle Bridge Deck Panels and Connections of Precast Ultra-High-Performance Concrete: Experimental Evaluation.” *Transportation Research Record* 2251 (1): 82–92.
8. Aaleti, S., J. Heine, and S. Sritharan. 2012. “Experimental Evaluation of UHPC Piles with a Splice and Pile-to-Abutment Connection Performance.” In *The PCI Convention and National Bridge Conference Proceedings, Sept. 29–Oct. 3, 2012, Nashville, TN*. Chicago, IL: PCI. CD-ROM.
9. Graybeal, Benjamin A. 2010. “Behavior of Field-Cast Ultra-High Performance Concrete Bridge Deck Connections under Cyclic and Static Structural Loading.” Report FHWA-HRT-11-023. McLean, VA: FHWA.
10. Carbonell Muñoz, Miguel A., Devin K. Harris, Theresa M. Ahlborn, and David C. Froster. 2013. “Bond Performance between Ultrahigh-Performance Concrete and Normal-Strength Concrete.” *Journal of Materials in Civil Engineering* 26 (8): 04014031.
11. Aaleti, Sriram, and Sri Sritharan. 2017. “Investigation of a Suitable Shear Friction Interface between UHPC and Normal Strength Concrete for Bridge Deck Applications.” InTrans project 10-379. Ames, IA: Iowa Department of Transportation.
12. ASTM Subcommittee C09.25. 2013. *Standard Test Method for Bond Strength of Epoxy-Resin Systems Used with Concrete by Slant Shear*. ASTM C882/C882M-13a. West Conshohocken, PA: ASTM International. https://doi.org/10.1520/C0882_C0882M-13A.
13. Crane, Charles Kennan. 2010. “Shear and Shear Friction of Ultra-High Performance Concrete Bridge Girders.” PhD diss., Georgia Institute of Technology.
14. Jang, Hyun-O., Han-Seung Lee, Keunhee Cho, and Jinkyu Kim. 2017. “Experimental Study on Shear Performance of Plain Construction Joints Integrated with Ultra-High Performance Concrete (UHPC).” *Construction and Building Materials* 152: 16–23.
15. ASTM Subcommittee C09.61. 2017. *Standard Test Method for Splitting Tensile Strength of Cylindrical Concrete Specimens*. ASTM C496/C496M-17. West Conshohocken, PA: ASTM International. https://doi.org/10.1520/C0496_C0496M-17
16. ASTM Subcommittee C09.25. 2013. *Standard Test Method for Tensile Strength of Concrete Surfaces and the Bond Strength or Tensile Strength of Concrete Repair and Overlay Materials by Direct Tension (Pull-off Method)*. ASTM C1583/C1583M-13. West Conshohocken, PA: ASTM International. https://doi.org/10.1520/C1583_C1583M-13.
17. Hussein, Husam H., Kenneth K. Walsh, Shad M. Sargand, and Eric P. Steinberg. 2016. “Interfacial Properties of Ultrahigh-Performance Concrete and High-Strength Concrete Bridge Connections.” *Journal of Materials in Civil Engineering* 28 (5): 04015208.
18. Ronanki, Vidya Sagar, David I. Burkhalter, Sriram Aaleti, Wei Song, and James A. Richardson. 2017. “Experimental and Analytical Investigation of End Zone Cracking in BT-78 Girders.” *Engineering Structures* 151: 503–517.
19. Burkhalter, David Isaac. 2016. “End Zone Design for Alabama Deep Prestressed Girders.” MS thesis, University of Alabama.
20. CEB (European Committee for Concrete). 1993. *CEB-FIP Model Code 1990: Design Code*. CEB bulletin 213/214. London, UK: Telford.
21. ACI (American Concrete Institute) Committee 318. 2014. *Building Code Requirements for Structural Concrete (ACI 318-14) and Commentary (ACI 318R-14)*. Farmington Hills, MI: ACI.
22. ASTM Subcommittee C09.25. 2003. *Standard Test Method for Bond Strength of Adhesive Systems Used with Concrete as Measured by Direct Tension (Withdrawn 2010)*. ASTM C1404/C1404M-98. West Conshohocken, PA: ASTM International.

Notation

C	= cohesive strength
d_b	= diameter of reinforcement
f'_c	= concrete compressive strength
f_t	= tensile strength
h	= girder height
K_m	= tensile stiffness
K_u	= shear stiffness
L	= length of girder
μ	= coefficient of friction

About the authors



Vidya Sagar Ronanki, PhD, is currently a bridge designer at T. Y. Lin International, in Bellevue, Wash. At the time of writing the paper, he was a PhD candidate in the Department of Civil, Construction and Environmental Engineering at the

University of Alabama in Tuscaloosa.



Sriram Aaleti, PhD, is an associate professor in the Department of Civil, Construction and Environmental Engineering at the University of Alabama. He is a voting member of the PCI Pile Producers Committee and the ACI 239A and ACI 239C committees on ul-

tra-high-performance concrete. His research interests include large-scale testing, ultra-high-performance concrete, precast/prestressed concrete structures, and behavior of concrete structures under earthquake loading.



J. P. Binard, PE, is the owner of Precast Systems Engineering in Exmore, Va. He has more than 15 years of design experience in the precast/prestressed concrete bridge industry. He is the current chair of the PCI UHPC Bridge Subcommittee of the Bridges

Committee and is past chair of the PCI Pile Producers Committee.

Abstract

Ultra-high-performance concrete (UHPC) is an engineered cementitious material with superior mechanical and durability properties compared with normalweight concrete (NWC). By taking advantage of these enhanced properties, a long-span hybrid girder design using standard girder shapes with UHPC in the end zone regions is proposed. Experimental studies were carried out to investigate the behavior of a UHPC-to-NWC interface with 0.2 in. (5 mm) roughness under shear and flexural loading. The results of the experimental studies were used to calibrate the necessary parameters required for developing a three-dimensional (3-D) finite element analysis (FEA) model for a hybrid girder. Structural performance of a 205 ft (62.5 m) long, 95 in. (2400 mm) deep Precast Concrete Economical Fabrication Committee standard bulb-tee (PCEF-95) hybrid girder was investigated using 3-D FEA models and compared with a girder designed with NWC. The hybrid girder exhibited better performance in terms of end zone cracking compared with the traditional concrete girder. Significant reduction in shear and end zone reinforcement was achieved in the hybrid girder compared with the NWC girder. The details regarding the feasibility of the proposed hybrid girder concept, the results from the interface tests, and the FEA study are presented in this paper.

Keywords

FEA, FEA model, finite element analysis, finite element analysis model, I-girder, interface behavior, long-span girder, prestressed girder, UHPC, ultra-high-performance concrete.

Review policy

This paper was reviewed in accordance with the Precast/Prestressed Concrete Institute's peer-review process.

Reader comments

Please address any reader comments to PCI Journal editor-in-chief Emily Lorenz at elorenz@pci.org or Precast/Prestressed Concrete Institute, c/o PCI Journal, 200 W. Adams St., Suite 2100, Chicago, IL 60606. [P](#)